Journal of the Indian Chemical Society 100 (2023) 100930

Contents lists available at ScienceDirect

Journal of the Indian Chemical Society

journal homepage: www.journals.elsevier.com/journal-of-the-indian-chemical-society

Magneto recyclable, green fabricated Fe_3O_4 nanorods on photo responsive of textile dye degradation and identification products by LC-MS

K. Sundaresan [a,*], S. Mohan [b,**], M.S. Manojkumar [c], Sakthisaravanan [d], M. Veera Raja [e], Mohd Shkir [f,g,h], H Elhosiny Ali [f,g,i]

[a] Meenakshi Ramasamy College of Arts and Science (Affliated to Bharathidasan University), Thathanur, 621804, Tiruchirapalli, TN, India
[b] Vivekanandha College of Arts and Sciences for Women (Autonomous), Tiruchengode, Namakkal - 637 205, TN, India
[c] Vivekanandha College of Engineering for Women (Autonomous), Tiruchengode, Namakkal - 637 205, TN, India
[d] RVS Engineering College, Coimbatore, Tamil Nadu, India
[e] PG Department of Physics, GTN Arts College Dindigul, 624 005, Tamil Nadu, India
[f] Research Center for Advanced Materials Science (RCAMS), King Khalid University, Abha, 61413, P.O. Box 9004, Saudi Arabia
[g] Department of Physics, Faculty of Science, King Khalid University, P.O. Box 9004, Abha, Saudi Arabia
[h] University Center for Research & Development (UCRD), Chandigarh University, NH95,Chandigarh-Ludhiana Highway, Gharuan, Mohali, Punjab, 140413, India
[i] Physics Department, Faculty of Science, Zagazig University, 44519 Zagazig, Egypt

ARTICLE INFO

Keywords:
X-ray techniques
Nanocrystalline materials
FTIR
Electron microscopy
Photo catalysis
Textile dyes

ABSTRACT

Prior to being released towards water sources such as rivers, lakes, and groundwater, the efficient technique of removing color out textile effluents seems to have become widely used. Such contaminants are extremely difficult for traditional wastewater treatment methods to completely eliminate. This innovative development of phytonutrients uses Fe_3O_4 nanorods, that have been employed as photocatalytic to change substrate colors in the aqueous layer when exposed to light. Given prominence was adopted to incorporate phytonutrients with Fe3O4 nanorods. The degradation of the methyl violet colour has been acknowledged by the depletion of the UV light (UV) absorption edge that also originated at 581 nm. The significant colour expulsion of the Fe3O4 nanorod was proved to really be 97% after 60 min. The findings demonstrate that ecologically responsible Fe_3O_4 nanorods are immensely beneficial in the photocatalytic reaction of harmful pollutants.

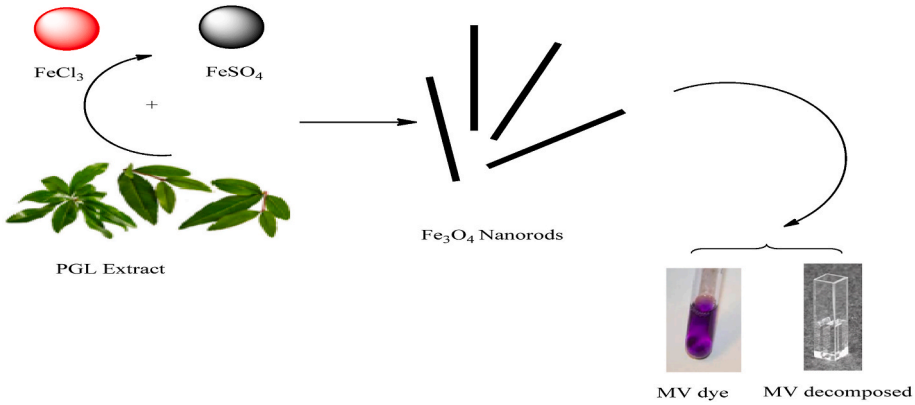
1. Introduction

In this materialistic society, first most highly toxic modern toxins are assimilated in the raw material to considerable extent being used nutrition, skincare, textiles, paper and cardboard sectors for purely aesthetic reasons. The vast numbers of them are outright dangerous that also embodies a remarkable threat to the current condition of the ecosphere. The dyes also were extensively employed in dye manufacturing [1] so upon intravenous mixture that leads to serious carcinogenicity and melanoma ailments [2]. Primarily, there seem to be various physicochemical strategies like as membrane filtration, bio-sorption on functionalized but also layer separation process. Magnetic nanoparticles (MNPs) are the foremost nanoscale materials with many practical applications such as ferrofluids, biosensors, catalysts, separation processes and environmental remediation. Especially, Fe_3O_4 (ferric oxide) belonging to the class of metal oxides was very well known for its unanimous photo catalytic and photo-oxidizing capacities. In Great Plains appealing iron oxide nanoparticles (Fe_3O_4 NRs) have indeed been adhered in distinctive sectors, such as validation and detachment of amino acids to continue improving the sensitivity of magnetic resonance imaging. (MRI), immunoassay and targeted drug delivery [3,4]. In part due to this, the consumption of the nanostructures has indeed adhered in a good deal with the consideration in the domain of Photocatalysts [5], polymer electrolyte membrane fuel membrane but also biosensor [6]. Likewise, a few really iron oxides and their matrix have revealed as a great tool for colour corruption by adsorbent [7,8] because of their substantial surface area to the volume ratio and diverse nanostructure materials.

Up to this point, various approaches have really been developed for the fabrication of Fe_3O_4 NRs, for solvothermal, ultrasonication, micro-

* Corresponding author.
** Corresponding author.
E-mail addresses: sundarphd21@gmail.com (K. Sundaresan), mohans@vicas.org (S. Mohan).

https://doi.org/10.1016/j.jics.2023.100930
Received 30 October 2022; Received in revised form 11 January 2023; Accepted 2 February 2023
Available online 8 February 2023
0019-4522/© 2023 Indian Chemical Society. Published by Elsevier B.V. All rights reserved.



Scheme 1. represents for the degradation of methyl violet using the nanorods.

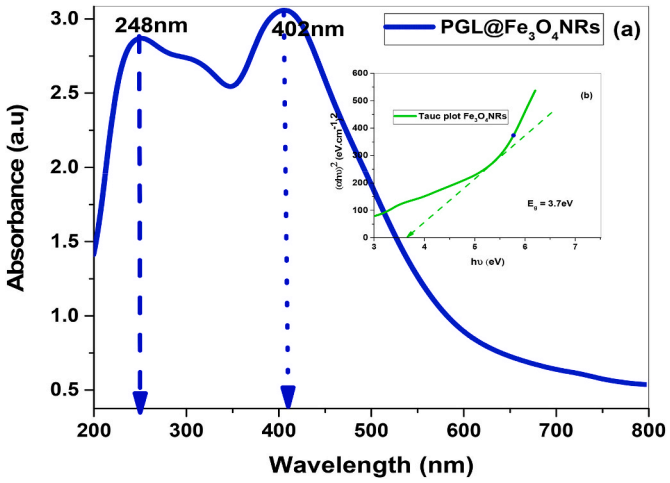


Fig. 1. (a) Electronic absorption spectra for Flavonoids @ Fe_3O_4 NRs using green route **(b)** In-situ of energy gap of Flavonoids @ Fe_3O_4 NRs.

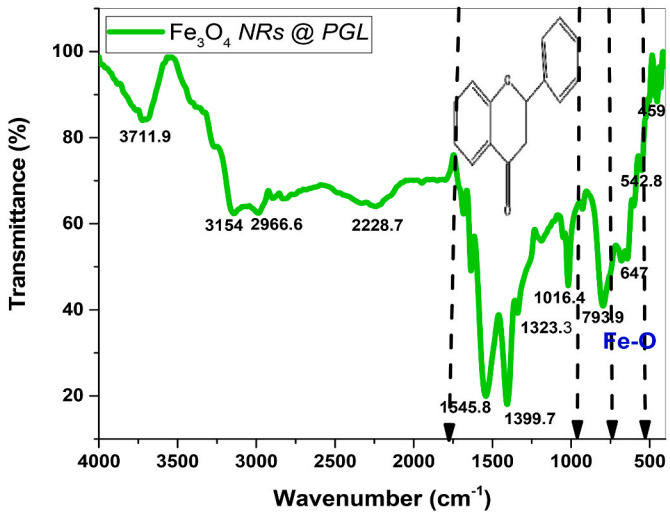


Fig. 2. Functional group analysis of flavonoids containing Fe3O4 NRs by FTIR spectrum.

emulsion, electrochemical, sol-gel and co-precipitation approaches [9, 10]. The sustainable green encapsulation has been used to fabricate Fe3O4 NRs because of its numerous advantages over biological and physicochemical strategies, such as the feature in that it doesn't use conceivably hazardous materials as well as being renewable, environmentally friendly, and cost-effective [9,10]. It uses readily accessible bioactive compounds from plants. One-dimensional Fe_3O_4 nanostructures have been high-lighted for many applications due to unique properties such as high specific surface area, single-crystal structure, high transparency, high electron mobility, large exciton binding energy (~ 60 meV), piezoelectricity and biocompatibility. In addition that Fe3O4 nanostructures-like nanowires, nanotubes and nanorods possess high surface-to-volume ratio and high areal density which can supply an electron transportation path. Particularly, Nanorod materials possess great anisotropic with exceptional magnetic behavior, which increase substrate combustion efficiency for waste water treatment compare to various metal oxide compounds like as ZnO NRs, CeO2 NRs and grpahene oxide doped ZnO NRs and so on [11–14].

Punica grantum leaves of the plant have been used as they would be widely obtainable. The pomegranate (Punica granatum) seems to be the prevailing hybrid of multiple species comprising the Punicaceae relatives. The phytoconstituents reveal in this plant extract of leaves encompasses triterpenic acids, alkaloids, tannins, flavonoids [15]. These phytochemical constituents play a role as stabilizing and capping agents and refine metal oxide nanoparticles by chemical reduction. According to our expertise, none research upon that usage of P. granatum leaves in the production of Fe_3O_4 NPs has been done so far.

The proposed approach has used a promising strategy for perhaps the first time; it places an emphasis on incorporating as well as employing flavonoid @ Fe_3O_4 NRs and highlighting one's photocatalytic investigation, synergist action upon methyl violet (MV) colour eviction in a watery medium.

1.1. Experimental

Punica grantum leaves, which act as functionalization agents, being gathered from the botanical herbal garden at Annamalai University in Tamil Nadu, India. All of the metal precursors, including $NaCOOCH_3$ > 99.9%, $FeCl_3.6H_20$ > 99%, NaOH > 99.9% and methyl violet fabric dye, were received from Sigma Aldrich. Without additional sanitization, the prescribed chemicals were used in deionized water.

1.2. Separation of functionalization agent (SFA)

5 g of powdered punica grantum leaf (PGL) were extracted solublely in a Soxhlet apparatus using a mixture of 50% methanol and 35% HCl. The acquired methanolic extracts subsequently neutralised with 0.3 mol of Sodium carbonate provisions, and so when petroleum ether and ethyl acetate were being separated, they have been triple-emptied and also the upper part disappeared. Punica grantum leaf extract (PGL), which has been fractionalized, has been eluted by proclivity. Five partitions was fractionalized using column chromatography from the 30 ml portion of

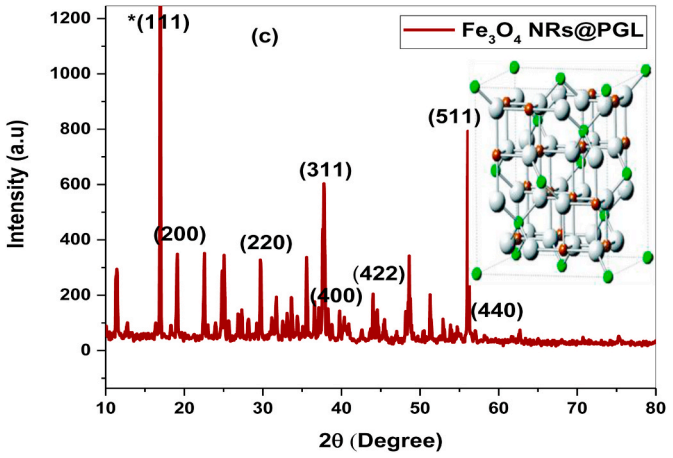


Fig. 3a. Crystallite structure identification by powder X-ray analysis.

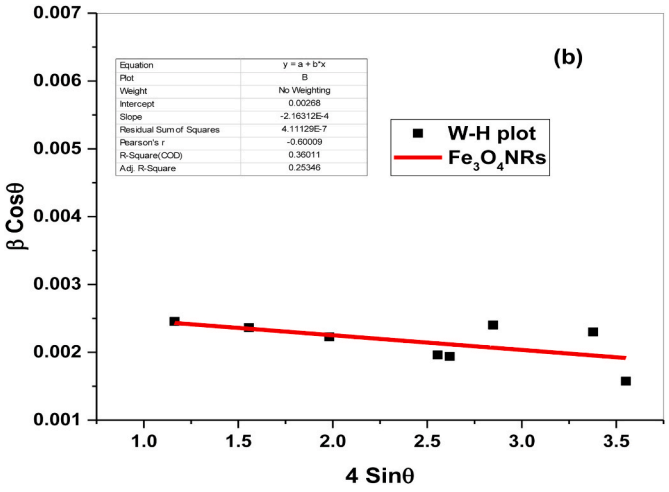


Fig. 3b. Williamsons Hall plot of Fe_3O_4 NRs.

the collected component. The acquired flavonoids isolates was evaluated by adding 0.5 ml hydroxide, and the extricated assays was homogenized at temperatures. It was evident that the PGL isolate used to have a yellow colour, indicating confirms the existence of flavonoids [16].

1.3. Construction of magneto recyclable Fe_3O_4 photocatalyst

A cheap and ecologically responsible strategy has been employed to construct Fe_3O_4 MNRs. The traditional method has been employed but probably adapted [17]. The construction of 3 g of $FeCl_3.6H_20$ with 5.56 g of sodium acetate was inserted as a bio-catalytic agent (flavonoid 50 ml) then vigorously agitated by 2 h at 80 °C. As an outcome, the homogeneous slurry assumed on such a block color, as well as the block products was subsequently obtained & separated as seen in Scheme 1.

1.4. 4Photocatalytic responsive of methyl violet (MV) dye degradation

The photo catalysis platform has examined the effects of flavonoid@Fe_3O_4 NRs on textile dye removal. 50 ml of 0.1 M MV dye combined with 10 mg of Fe_3O_4 NRs were used in the experiment, which was then exposed to UV light. A control (MV) set was also employed in the absence of a catalyst. The essence of the reaction medium was to offer desorption stability for repetitive exposure. Eventually, the chromphoric group started splitting by UV light. While also exposed to an accelerator (a mercury lamp of 120 W) for various periods of time [18]. Decomposition of the color was represented by a sharp reduction in the absorption maximum at (max = 581 nm), as illustrated in Fig. 6. (a).

2. Results and discussion

Electronic absorption bands of embedded Fe_3O_4NRs have been obviously two shoulder bands were noticed like band I (Flavonoid) at 248 nm. The characteristic peaks for flavonoids and other phenolic compounds traditionally are located in the range of 210–290 nm and band II (Fe–O) at 402 nm was immobilised flavonoid @ Fe_3O_4 NRs was identified in Fig. 1 (a). Identical findings also backed up [19,20]. This is as an outcome of Fe_3O_4 NR development seeming to be dependent on the nucleation and growth pathway [16]. In relation to its Fourier transform infrared [FT IR] spectrum clearly demonstrated that perhaps the carbonyl aggregating flavonoids component had been in strong coordinating relationship. The energy band gap of Fe_3O_4 NRs in situ is revealed by Tauc's correlations in Fig. 1(b).

$$\alpha h\nu = C(h\nu - E_g)^2 \quad (1)$$

Flavonoid@Fe3O4 NRs have been revealed to possess a binding energy of 2.7 eV, which has been caused by a substantial photonic attraction and a higher electrode potential of +33 eV.

According to Fig. 2, the FTIR characteristic peak for Fe_3O_4 nanorods was extended greatly at 3421, 2925, 1626, 1407, 1234, and 1067 cm^{-1}. Unexpectedly, further groups at 590 & 622 cm^{-1} are attributed to the typical extended oscillations of the Fe–O bond [21]. The FTIR characteristic then reveals the significant role of the flavonoids group in bioactive molecules, which adjusts the flavonoids at Fe_3O_4NRs that reduces Fe^{3+}/Fe^{2+} metal ions.

The powder X-ray diffraction (XRD) analysis was employed to determine the crystalline phase composition of Fe_3O_4 NRs. The XRD characteristic of Fe_3O_4 NRs obtained using the flavonoid extract is shown in Fig. 3a (PGL). Fig. 3b shows the Williamson hall plot of dislocation density. The cubic inverse spinal structure of Fe_3O_4NRs (JCPDS # 76–045) has been well correlated to six relatively strong reflections peak that also are present in (111), (200), (220), (311), (400), and (440) in the XRD patterns of the Fe_3O_4NRs, which facilitates the construction of Fe_3O_4 NRs. The Scherrer equation was employed to determine the crystallite size [21,22].

$$D = 0.9\lambda / \beta \cos\theta \quad (2)$$

The average crystallite diameter of the predicted Fe_3O_4 NRs approximately 17.7 nm, as well as the microstrain of the Fe_3O_4 NRs was estimated using algorithm.

$$\varepsilon = \beta \cos\theta/4 \quad (3)$$

Dis-location density is derived this equation

$$\delta = 1/D^2 \quad (4)$$

The dislocation density of Fe_3O_4 NRs was estimated to be 8.75 × 10^{15}, and the micro strain was determined to be 0.807 × 10^{-3}. Therefore could assume from of the outcomes that its crystal field distracts and potentially active strain rate of degree of crystallinity also facilitated in the color cleanup process [23].

The dimensions and Morphologies of the Fe_3O_4 NRs have been stated to really be wire, rod-shaped through the scanning electron microscopy (SEM), and transmission electron microscopy(TEM) appraisal. Fig. 4(a) and **(b)** show multiple magnifications of the SEM micrographs of the Fe_3O_4 NRs that also strongly indicates wire-like structures Fig. 4(c) represents TEM image of derived Fe_3O_4 NRs that also clearly presented rod-like configuration. The mean size of the nanorods has indeed been evidenced 15–20 nm. The rod like configuration of Fe_3O_4 nanoparticles was improving the resilience ROS radicals that empower with photo

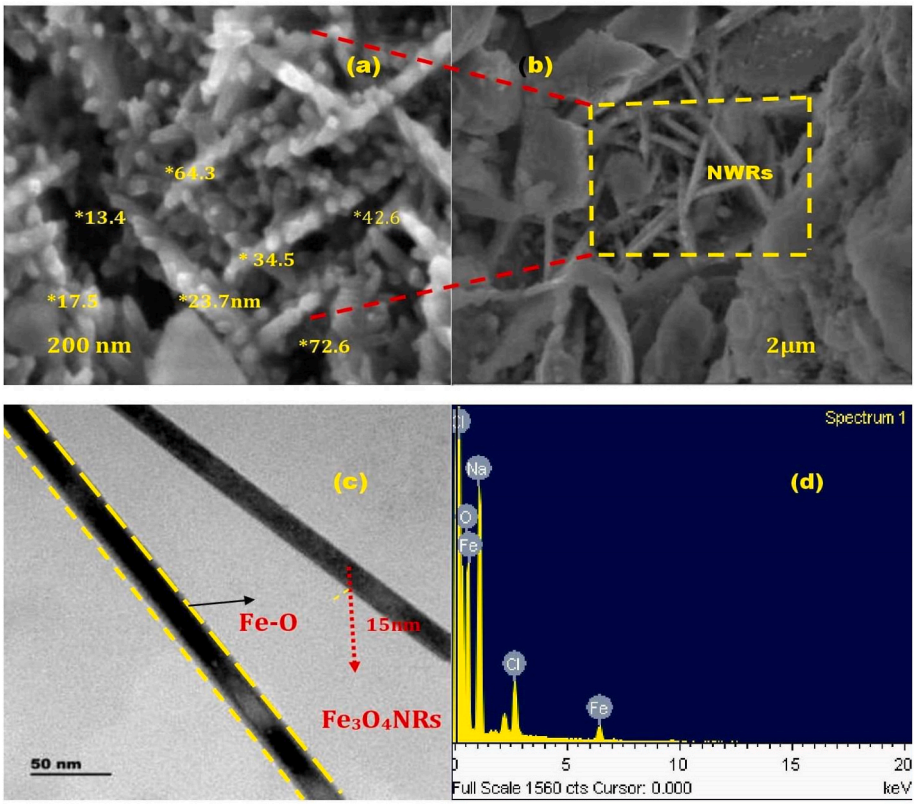


Fig. 4. (a) and (b) various magnification of Fe_3O_4 nanowire by SEM (c) HR-TEM image of Fe_3O_4 nanorods (d) Elemental composition spectrum.

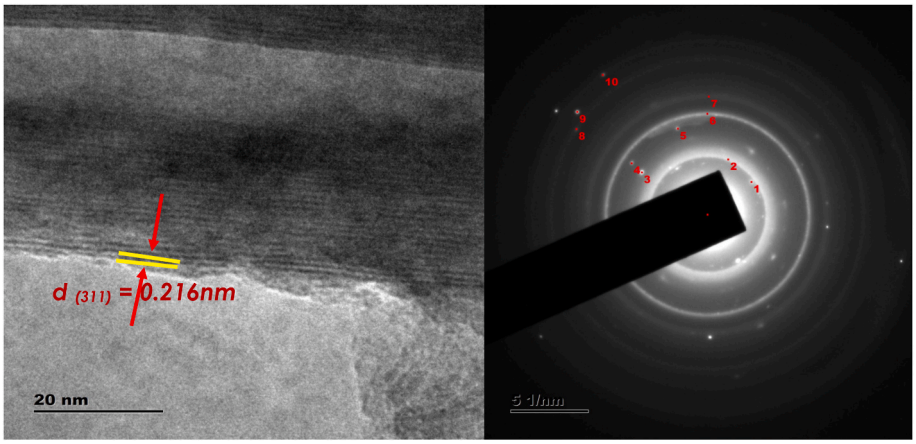


Fig. 5. (a) HRTEM profile (b) SEAD pattern of synthesized Fe_3O_4 nanorods.

catalytic activity [24,25]. The EDS assessment of the Fe_3O_4 is illustrated in Fig. 4(d) that also evidently reveals the presence of Fe and O in the material surface and also other susceptible peaks were Na, Cl, K found present in PGL extract.

HRTEM image Fig. 5 (a) has given us further insight into the microstructure and crystallinity of as-prepared Fe_3O_4 nanoparticles. The clear and uniform lattice fringes confirmed that the spherical particles are highly crystallized. The lattice spacing of 0.216 nm, corresponds to (311) planes of Fe_3O_4 nanocomposites. The results show that the dominant faces of Fe_3O_4 spheres are (311). The SAED pattern has been obtained by directing the electron beam perpendicular to one of the spheres. The hexagonal symmetry of diffraction spots pattern shown in Fig. 5(b) confirmed that the nanorods are well crystalline, and its face is indexed to (311) planes. Both HRTEM image and SAED pattern confirmed that the prepared Fe_3O_4 nanorods are single crystals.

Fig. 6 (a) reveals that pore space and distribution of pores has been obtained by Barrett-Joyner-Halenda evaluation. The observations evidenced that fabricated Fe_3O_4 NRs appeared to possess a massive specific surface area of 114.2 m^2 and 166.6 $m^2\ g^{-1}$ with 10.30 nm pore diameter and 0.328 cm^3/g high porosity. This will also be potent for photocatalysts execution to obey Methyl violet dye degradation [Fig. 6b]. represents the isotherms architects plot of the derived Fe_3O_4 NRs [26].

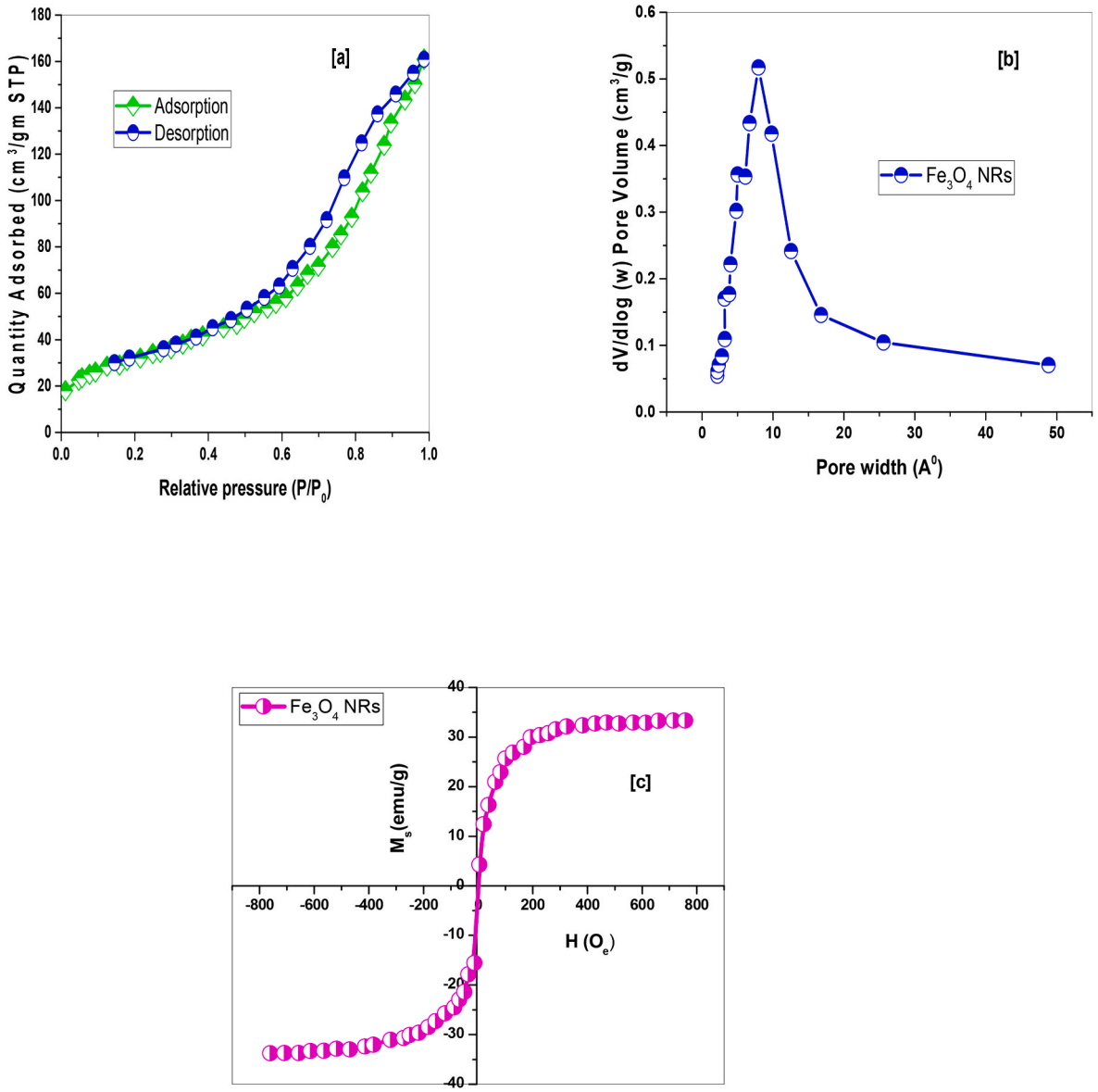


Fig. 6. **(a)** adsorption-desorption isotherm curve **(b)** pore distribution graph **(c)** M − H loops of Fe_3O_4 NRs at room temperature.

Fig. 6 (c) proves the hysteresis loop validating the ferromagnetism of Fe_3O_4 NRs with saturation magnetization (Ms) value of about 38 emu/g, the coercive force (Hc) of 265.48 G and magnetic remanence (Mr) of 2.62 emu/g. These magnetic properties would then acknowledge to the composite materials that also are to be used in photo catalytic attentive of fabric dye degradation and also possessing an excellent reusable assets.

Fig. 7(a) and (b), which represents the existence of different bio-moieties onto the Fe_3O_4 and surface of Fe_3O_4 modified with PGL extract. The binding energy values for the main peak maxima Fe 2p 3/2 and 2p1/2 were found at 712.1 and 726.5 eV, respectively (Fig. 7(a)). Our results are in good agreement with the values reported for Fe3O4 and surface modified Fe3O4 in the literature [27]. The main C1s peak at 284.6 eV (Fig. 7(b)) can be assigned to the carbon atoms within phenyl and carbonyl groups residues of the polyphenolic constituents. The O1s core level decomposed into three chemically distinct components at 529.8 eV denotes the existence of carboxylate groups. The N1s core level centred at 398.5 attributes the amine groups present in the indole derivatives and protein moieties. From these results, we speculate that the Fe3þ ions are in strong coordination with water-soluble heterocyclic metabolites of PGL. During nucleation, these active bioconstituents could be preferentially adsorbed onto the surface; also it controls the nucleation position through special confinement [28].

2.1. *Effect of contact time*

Fig. 8 (a) represents the modifications in the Methyl violet absorption bands during photodegradation with Fe_3O_4 at various exposure times differing from 0 to 60 min. Upwards of 97% of the MV is diminished within 90 min existed synchronously with expanding illumination time. The hypsochromic shift could be prompted by an N-demethylation stage. The absorbance signals at 581 nm have dropped significantly, that also demonstrates that the complete conjugated chromophore component of Methyl violet (MV) has been excluded [29].

2.2. *Effect of pH*

The effect of different pH (4, 6, 8, and 10) regard on the defilement

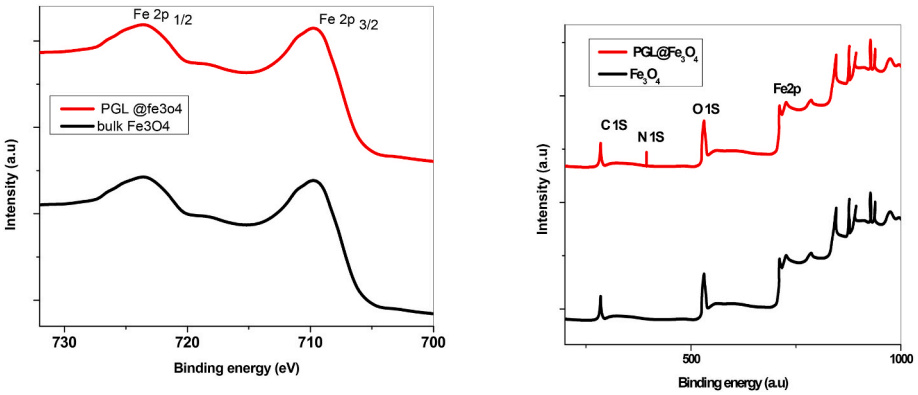


Fig. 7. (a) XPS spectrumof Fe 2p (b) survey scan spectrum of Fe_3O_4 and PGL @ Fe_3O_4 NRs.

efficiency of MV was investigated, which is shown in Fig. 8(b). The customary pH worth of MV course of action was considered to be 5.8. The pH regard was changed including debilitate HCl or debilitate NaOH reply for the assessment. The effect of pH on the corruption of MV was examined by changing the pH from 4, 6, 8 and 10 at a nice proportion of catalyst (10 mg/L) and consistent MV obsession (10 mg/L). Fig. 8(b)

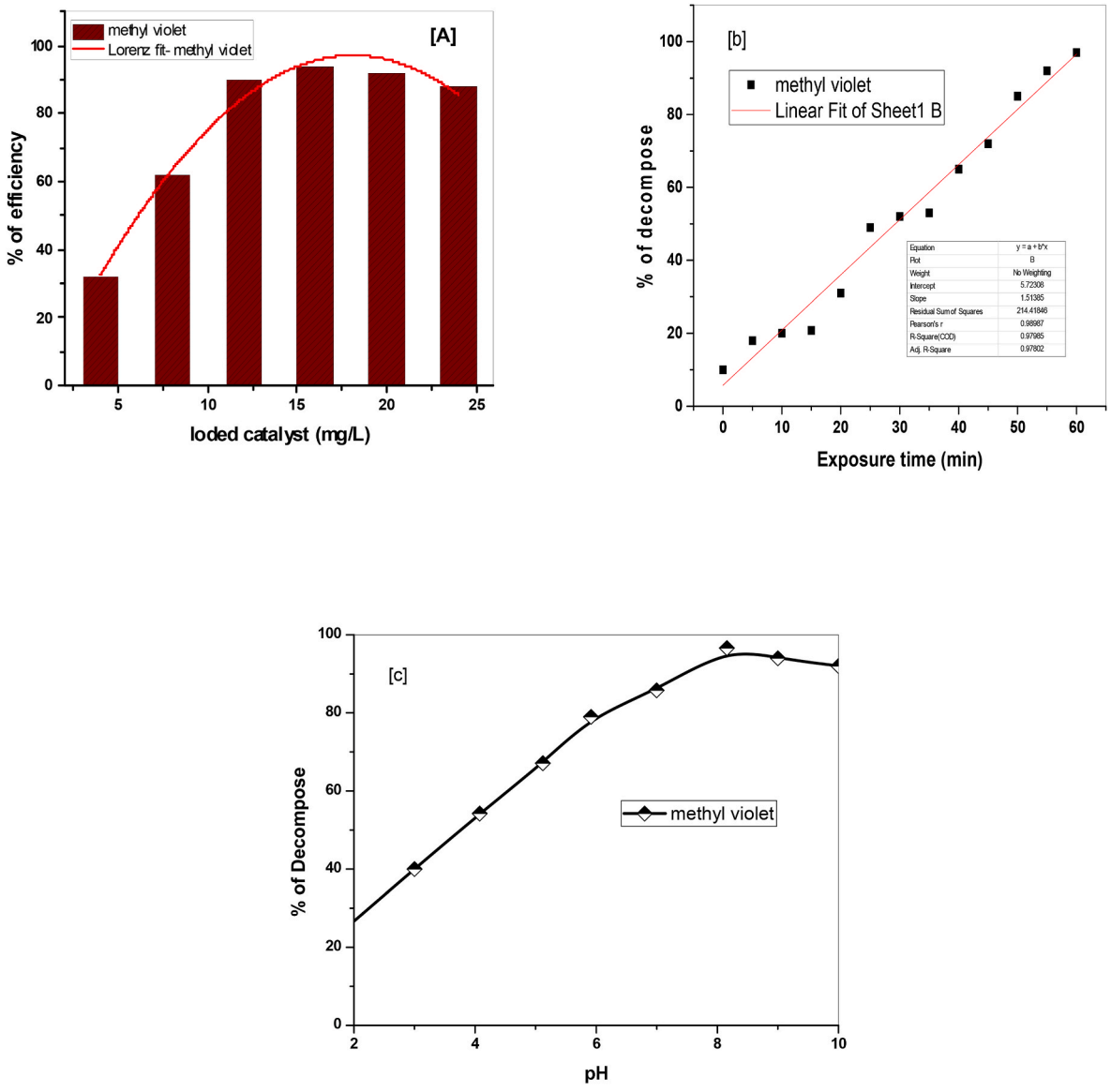


Fig. 8. (a) catalyst dose **(b)**effect of exposure time **(c)** effect of pH of methyl violet decompose.

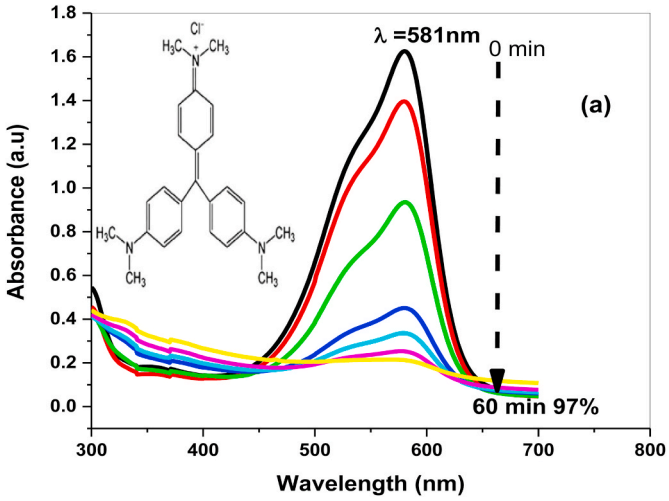


Fig. 9a. Different time exposure of methyl violet dye degradation curve via photocatalysis method.

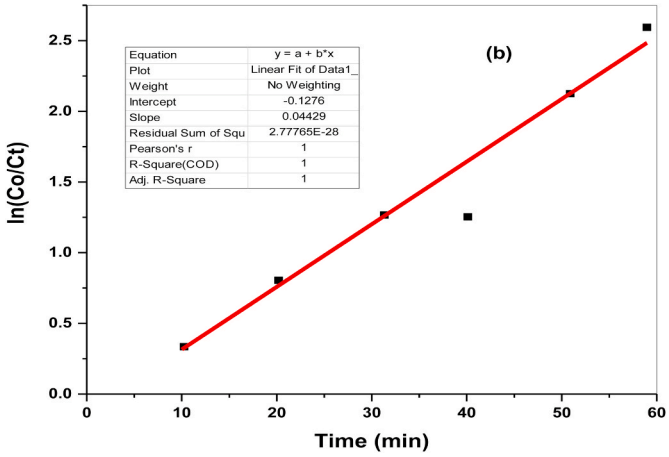
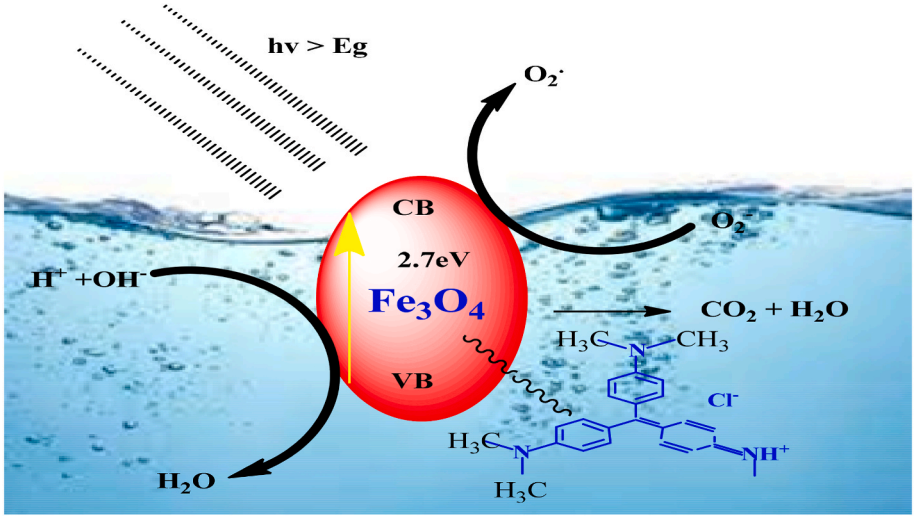


Fig. 9b. kinetic plot of Fe_3O_4NRs via green route.



Scheme 2. profile of photo catalytic mechanism of methyl violet dye removal on Fe_3O_4 nanorods.

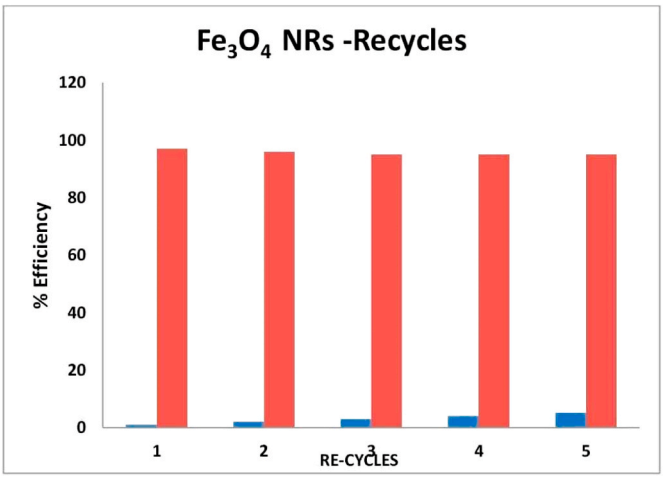


Fig. 9c. Reusability of Fe_3O_4 NRs photocatlyst after five cycle exposure.

shows the effect of pH on the photodegradation of MV plan. At pH 5.8, it is seen that the maintenance band of the MV is 581 nm. Since, the assortment from significant violet changes to exhausting, there is a fast reducing with a slight hypochromic shift which is found at 581 nm, and there is no new maintenance band in the UV range. It shows that there would be a cleavage of the framed chromophore development of the MV which would have occurred considering the plan of N-demethylated intermediates. In the acidic pH 5, the maintenance top at 581 nm

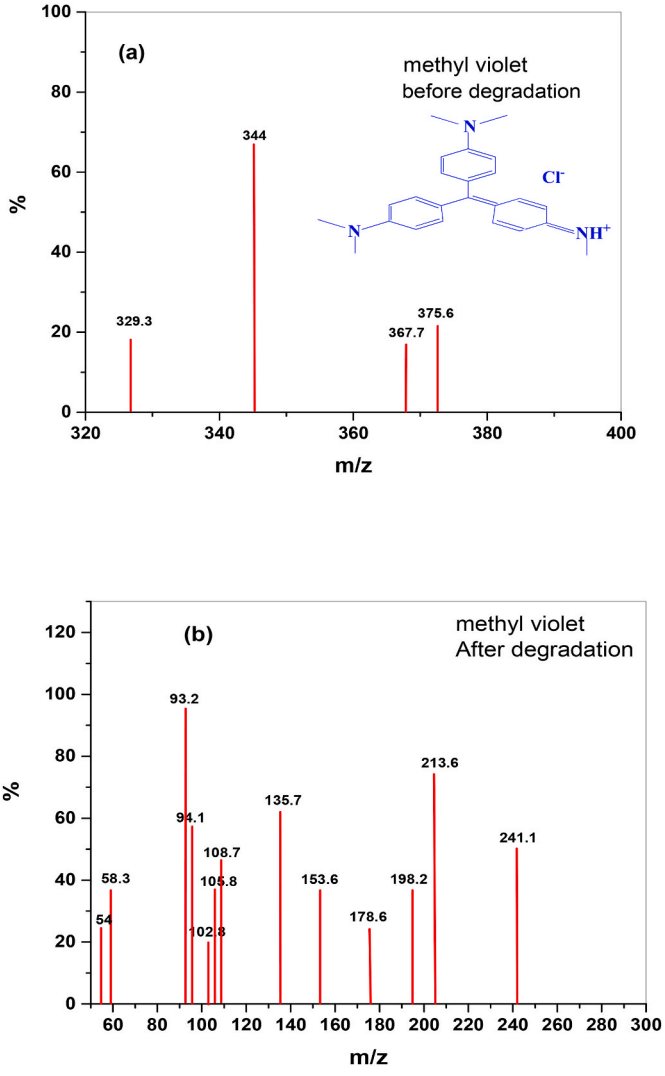


Fig. 10. (a) untreated samples (without catalyst) **(b)** treated samples (with catalyst).

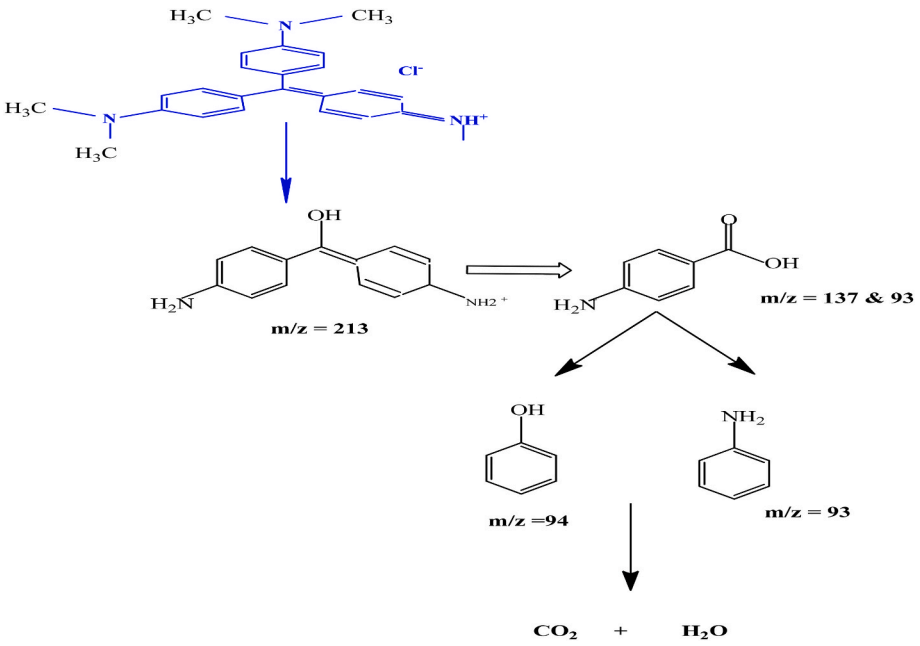


Fig. 11. mechanism path way methyl violet degradation on Fe_3O_4 reusability catalyst.

avowed that there is adsorption of MV on Fe_3O_4 stimulus surface. It is found that defilement works out (99.53%) inside 60 min at pH 6. The electrons in the conduction band can be gotten by the dissolvable O_2, and the openings can be gotten by the surface hydroxyl, these cycle achieving the advancement of hydroxyl fanatic species (•OH), which are successfully made by oxidizing more hydroxide particles in acidic plan. As such, the capability of the debasement cycle is worked on in the acidic medium, especially at pH 6. Thusly, the acidic medium endowments the complete defilement of MV on the external layer of the stimulus.

2.3. Effect of catalyst dosage

The amount of photocatalyst is another factor affecting the performance of the photocatalyst. The photo-catalytic study was conducted under the following conditions: a source of irradiation, visible light, type of photocatalyst (Fe_3O_4 photocatalyst), the weight of photocatalyst (10 mg–50 mg) and concentration of MV dye solution (2×10^{-5} M). The effect of the loading of the Fe_3O_4 heterogeneous photocatalyst on the degradation of MV dye is shown in Fig. 8(c). The results reveal that the photocatalytic activity increased 80–95% after 60 min by increasing the weight of the Fe_3O_4 photocatalyst from 10 mg to 50 mg/L due to increased. The degree of decomposition reaction increases with the increase in the reactive sites on the catalyst, beyond which, it shows that the degradation process is reduced, because of the scattering of light. There is a decrease in the penetration of light in the solution. When the amount of catalyst is higher in the solution, the activated molecules get deactivated by the collision of the lower energy molecules thereby increasing the turbidity of the medium and reduction in penetration of light leads to decrease in the rate of the reaction. Also, when the photocatalyst absorbs the highest light; hence, the surface area becomes high, as a result of agglomeration at higher concentration of catalyst.

2.4. Kinetic model

The kinetic behavior of Fe_3O_4 nanorods on methyl violet dye was inspected by photo catalytic method (PCM) and LangmuirHinshelwood mechanism was followed:

$$\ln (C/C_0) = K_{app}t \quad (5)$$

The plot of the graph ln (C/C_0) vs time for the Fe_3O_4 NRs were rate constant which was found to be 0.0789 min^{-1} and also pseudo first order kinetic model was shown in Fig. 9b [30].

2.5. Mechanisms pathway

Fig. 9a shows that once the light is incident on the material, the excitation of electrons occurs from VB to CB, and forming the electron-holes in the VB. Furthermore the separation of charge and movement of produced charge carriers to surface ofFe_3O_4 layer and can be led to the redox process. The reactive oxygen (ROS) species of (h+) (VB) in Flavonoid@Fe_3O_4nanorodsis oxidation of MV to responsive intermediates radicals (*OH) that can convert into decomposition of water in Scheme 2 [3,21]. Fig. 9c showed that the reusability and stability of flavonoid@Fe_3O_4 NRs were highly stable were evaluated for five cycles with strong effective nature [2].

2.6. Determination of fragmentation products by LC-MS

Fig. 10 (a) and **(b)** shows that the LC-MS spectra of defilement consequences of methyl violet. General pathway for the defilement of methyl violet has been presented in plot 2. The debasement cycle occurs inside seeing ROS and for our circumstance, hydroxyl progressives are the huge one. Attack by hydroxyl fanatics came to fruition into methyl violet corruption as scholarly by the LC-MS spectra with huge cooperation saw as de-methylation attack by uncommonly open hydroxyl progressives onto methyl violet was provoked the lack of methyl pack yielding thing with regard 344.7 m/z. Further demethylation of this separated thing provoked the advancement of parts with *m/z* potential gains of 58.3 93.2, 94.1, 135.7, 178.6, 213.6 and 241.1 as presented in Fig. 10 (b). Thing with *m/z* regard 288 has been recognized as p-rosaniline which was formed by the lack of all methyl bunches [30,31] (see Fig. 11).

3. Conclusion

In accordance with the plan, the flavonoids @Fe_3O_4 NRs have been successfully obtained employing PG leaves extract in a more environmentally friendly manner. In this way, various logical representations of

the reusable and photo endurance of Fe_3O_4 NRs have been established. The strong dis-area thickness of 8.75×10^{15}, crystal field fascination, and adaptable oxygen species (AOS) constituent were also delivered to as fast response rates and simple to attain quickly in the color removal process, which contributed to the fascinating colour eviction of flavonoids @Fe_3O_4NRs were seen to be 97% at an hour period. The flavonoids @Fe_3O_4 NRs are potentially useful for contaminated water treaments, MRI, diagnostic devices, and other applications.

Declaration of competing interest

The authors declare that there is no conflict of interest regarding the research work reported in this manuscript.

Acknowledgment

The authors extend their appreciation to the Research Center for Advanced Materials Science (RCAMS), King Khalid University, Saudi Arabia, for funding this work under grant number RCAMS/KKU/013-22.

References

[1] M.J.K. Ahmed, M. Ahmaruzzaman, M.H. Bordoloi, RSC Adv. 5 (2015) 74645–74655.
[2] M. Atarod, M. Nasrollahzadeh, S.M. Sajadi, RSC Adv. 5 (2015) 91532–91543.
[3] F. Barahuie, D. Dorniani, B. Saifullah, S. Gothai, M.Z. Hussein, A.K. Pandurangan, P. Arulselvan, M.E. Norhaizan, Int. J. Nanomed. 12 (2017) 2361–2372.
[4] B.R. Hao, R. Xing, Z. Xu, Y. Hou, S. Gao, S. Sun, Adv. Mater. 22 (2010) 2729–2742.
[5] D. Astruc, F. Lu, J.R. Aranzaes, Angew. Chem. 117 (2005) 8062–8083.
[6] I. Chourpa, L. Douziech-Eyrolles, L. Ngaboni-Okassa, J.F. Fouquenet, S. Cohen-Jonathan, M. Souce, H. Marchais, P. Dubois, Analyst 130 (2005) 1395–1403.
[7] R. Mirzajani, S. Ahmadi, J. Ind. Eng. Chem. 23 (2015) 171–178.
[8] X.M. Liang, L.J. Zhao, RSC Adv. 2 (2012) 5485–5487.
[9] O.A. Attallah, E. Girgis, M.M. Abdel-Mottaleb, J. Magn. Mater. 399 (2016) 58–63.
[10] J.H. Wu, S.P. Ko, H.L. Liu, M.H. Jung, J.H. Lee, J.S. Ju, Y.K. Kim, Colloids Surf. Physico. Chem. Eng. Aspects 313–314 (2008) 264–267.
[11] AlaManoharV. Vijayakanth, S.V. Prabhakar VattikutiKi Hyeon Kim, Ceram. Int. 20 (15) (2022) 30695–30703.
[12] Ala Manohar, V Vijayakanth, SV Prabhakar Vattikuti, Ki Hyeon Kim, Mater. Chem. Phys., 126117.
[13] Ala Manohar, Vembakam Vijayakanth, SV Prabhakar Vattikuti, Panchanathan Manivasagan, Eue-Soon Jang, Krishnamoorthi Chintagumpala, Ki Hyeon Kim, ACS Appl. Nano Mater. 5 (4), 5847-5856.
[14] S.M.A. Rastialhosseini, A. Khayatian, R. Shariatzadeh, M. AlmasiKash, Appl. Phys. A 125 (2019) 829.
[15] I.O. Macdonald, A.S.A. Oludare, Life Sci. J. 7 (2010) 3.
[16] Sada Venkateswarlu, Bhajanthri Natesh Kumar, Bobbala Prathima, Yakkate Subba Rao, Nimmagadda Venkata Vijaya Jyothi, Arab. J. Chem. (2014), 09 – 006.
[17] Santhanam Mohan, Manickam Vishnudevan, Green processing synth 8 (2019) 895–900.
[18] Sumit Arora, Itankar Prakash, J. Tradition. Complemen. Med. 8 (2018) 476e482.
[19] Van Thuan Le, Van Dat Doan, Thi Thanh Nhi Le, My Uyen Do, Thu-Thao Thi Vo, Ha Huu Do, Dinh Quoc Viet, Vy Anh Tran, Mater. Lett. 283 (2021), 128749.
[20] S. Kaviya, Viswanathan B. SanthanalakshmiJ, J. Muthumary, K. Srinivasan, Spectrochim. Acta, Part A 79 (2011) 594–598.
[21] Cheera Prasad, KarlapudiS, P. Venkateswarlu, I. Bahadur, S. Kumar, J. Mol. Liq. 240 (2017) 322–328.
[22] SadaVenkateswarlu, Y. Subba Rao, T. Balaji, B. Prathima, N.V.V. Jyothi, Mater. Lett. 100 (2013) 241–244.
[23] A.S. Hassanien, B. Alaa, A. Aklcd, A.H. Sáaedi, CrystEngComm 20 (2018) 1716–1730.
[24] Azar Sadullahkhani, Iraj kazeminezhad, Jun Lu ormer Nur, Lars hulman, Magnus willander, RSC Adv. 4 (2014) 36940–36950.
[25] Abdelmajid Lassoued, Mohamed Saber Lassoued, Brahim Dkhil, Salah Ammar, Abdellatif Gadri, J. Mater. Sci. Mater. Electronic. (2018), https://doi.org/10.1007/10854-018-8819-4.
[26] Naresh Kumar Sethy, Zeenat Arif, Pradeep Kumar Mishra, Pradeep Kumar, Green Process Synth 9 (2020) 171–181.
[27] Y. Tuo, G. Liu, B. Dong, et al., Sci. Rep. 5 (2015), 13515.
[28] K.K. Cheng, P.S. Chan, S. Fan, et al., Biomaterials 44 (2015) 155–172.
[29] Adeel Ahmed Muhammad Usman Bing Yua, Xin Ding, YouqingShena QiaohongPenga, Hailin Conga, Adeel Ahmeda, Muhammad Usman, Bing Yua, b Xin Dinga, YouqingShena QiaohongPenga, Hailin Conga, J. Photochem. Photobiol., B: Biol. 202 (2020), 111682.
[30] M. Ahmaruzzaman Bhattacharjee, T.B. Devi, J. Nath, J. Photochem. Photobiol. Chem. 325 (2016) 116–124.
[31] M. Fayazi, S. Azizian, J. Mol. Liq. 224 (2016) 763–767.